PUM2 knockdown regulates the expression and alternative splicing of genes associated with myocardial fibrosis in H9C2 cells

ZILONG ZHANG[1*], HANGYU ZHOU[1*], DILIYAER ADILI[1], WEI ZHU[1], YONG LIU[1], WENZHENG ZHOU[2], ZHAO WANG[1] and JIE LI[1]

[1]Cardiac and Panvascular Medicine Diagnosis and Treatment Center, People's Hospital of Xinjiang Uygur Autonomous Region, Ürümqi, Xinjiang Uyghur Autonomous Region 830000, P.R. China; [2]Department of Orthopaedics, People's Hospital of Xinjiang Uygur Autonomous Region, Ürümqi, Xinjiang Uyghur Autonomous Region 830000, P.R. China

Received April 7, 2025; Accepted October 30, 2025

DOI: 10.3892/etm.2026.13089

Abstract. Myocardial fibrosis (MF) represents a major pathological alteration observed in the progression of numerous heart conditions. The presence of excessive MF is key in the progression of numerous heart diseases, which may lead to heart failure. Abnormal expression of pumilio RNA-binding family member 2 (PUM2), an RNA-binding protein, is a contributing factor in the development of a variety of diseases. The present study aimed to investigate how PUM2 affected the expression and alternative splicing of genes associated with MF in H9C2 cells, thus evaluating the role of PUM2 in this context. Inhibition of PUM2 expression in H9C2 cardiomyocytes was achieved through small interfering RNA transfection. Cell viability was assessed using a Cell Counting Kit-8 assay, while apoptosis was detected through flow cytometry. RNA-sequencing (RNA-seq) was utilized to analyze the differential gene expression profiles and alternative splicing events (ASEs) in H9C2 cells regulated by PUM2. Sequencing results were confirmed through reverse transcription-quantitative PCR. The results showed that a reduction in PUM2 levels inhibited cell viability without affecting apoptosis. RNA-seq analysis revealed notable changes in the expression of various genes associated with MF, including adrenomedullin, NDRG family member 4, phospholipid phosphatase 3, integrin subunit α 8, regulator of G protein signaling 2, cadherin 11, integrin subunit α 11 and transforming growth factor β-induced, following PUM2 knockdown. In addition, PUM2 regulated ASEs in genes associated with fibrosis progression, such as tropomyosin 1 and actinin α1. The present study revealed that PUM2 had a regulatory effect on alternative splicing and gene expression associated with MF, suggesting PUM2 as a promising molecular target for MF therapy.

Correspondence to: Professor Jie Li or Professor Zhao Wang, Cardiac and Panvascular Medicine Diagnosis and Treatment Center, People's Hospital of Xinjiang Uygur Autonomous Region, 23 South Xingfu Road, Ürümqi, Xinjiang Uyghur Autonomous Region 830000, P.R. China
E-mail: lijie090715@126.com
E-mail: xjzzqwz@163.com

*Contributed equally

Key words: myocardial fibrosis, pumilio RNA-binding family member 2, RNA-sequencing, differential gene expression, alternative splicing

Introduction

Myocardial fibrosis (MF) represents a key pathological change associated with the remodeling of myocardial tissue, characterized by an increase in the interstitial space within the heart muscle, primarily as a result of heightened deposition of extracellular matrix (ECM) components (1). This accumulation is largely driven by the activity of activated myofibroblasts, which serve a key role in the fibrotic process (2). As a consequence of MF, patients often experience a range of adverse cardiovascular effects, including an increase in myocardial stiffness, which can hinder the ability of the heart to relax properly during diastole, leading to ventricular diastolic dysfunction (3). Furthermore, MF can contribute to a decreased coronary flow reserve, impacting the capacity of the heart to receive an adequate blood supply during heightened activity (4). Globally, the annual incidence rate of MF is ~1.7% (5). Notably, MF affects >60% of patients with chronic heart failure and is a key predictor of adverse outcomes, including arrhythmias and sudden cardiac mortality, with 5-year mortality rates ranging from 40 to 60% (5,6). Current MF management involves renin-angiotensin-aldosterone system inhibitors, β-blockers and statins. While they may alleviate the symptoms of patients, these agents have demonstrated a limited efficacy in halting or reversing MF (7). Mechanistically, the complexity of the fibroblast response to injury and the pathophysiologic heterogeneity of MF pose challenges to the development of antifibrotic therapeutic strategies (8). To the best of our knowledge, currently, there is no ideal treatment for MF, thus novel therapeutic strategies need to be developed. In previous years, with the development of high-throughput sequencing technology, molecular targeted therapies have become a hotspot for the treatment of a number of diseases (9,10). The exact etiology of MF remains unclear, highlighting the importance of in-depth studies focusing on the molecular mechanisms of MF to identify novel therapeutic targets.

RNA-binding proteins (RBPs) are proteins that bind to RNA to regulate RNA metabolism (11). RBPs interact directly with single- or double-stranded RNA and are involved in post-transcriptional processes such as alternative splicing, RNA export, mRNA translation, RNA degradation and RNA stabilization to regulate gene expression (12-14). Dysfunctions in RBPs underscore a number of diseases. A previous study demonstrated that reducing the expression of CUGBP Elav-like family member 1 could notably ameliorate cardiac fibrosis (15). In addition, another study demonstrated that inhibition of cytoskeleton associated protein 4 expression led to an increase in the expression of TGF-β-stimulated fibroblast activation-related genes, which subsequently serves a role in the regulation of MF (16). Furthermore, it has been reported that polypyrimidine tract binding protein 1 promotes cardiac fibrosis by facilitating collagen deposition through the degradation of nuclear receptor 4A1 mRNA, followed by transcriptional repression of fatty acid binding protein 5 (17).

Pumilio RNA-binding family member 2 (PUM2), a member of the pumilio family, belongs to a group of RBPs that recognize sequences in RNA. PUM2 functions as a translational regulator during embryonic development and cell differentiation (18). PUM2 serves as a translational repressor that becomes increasingly active during the process of cellular senescence. Importantly, it functions as a negative regulator of both lifespan and the maintenance of mitochondrial homeostasis, meaning that the presence and activity of PUM2 can inhibit cellular processes that are key for longevity and the proper functioning of mitochondria, overall contributing to the aging process at a cellular level. Understanding the mechanisms by which PUM2 operates could provide insights into the complexities of lifespan regulation and the preservation of mitochondrial integrity (19). Aberrant expression of PUM2 is implicated in the progression of a range of diseases. Ding *et al* (20) demonstrated that, in cervical cancer, PUM2 promoted tumor progression by destabilizing tumor-suppressor mRNAs. A recent study found that PUM2 also exacerbated neuroinflammation and brain damage caused by ischemia-reperfusion (21). These findings demonstrate the capacity of PUM2 to drive pathological processes across tissues, suggesting it as a high-priority target for MF investigation. In MF-related studies, PUM2 serves as a regulatory hub for gene translation in fibrotic hearts of patients with dilated cardiomyopathy (22,23). *In vitro* experiments have demonstrated that knockdown of PUM2 inhibits TGF-β1-induced fibroblast activation (24). However, whether PUM2 contributes to cardiac fibrosis by regulating the expression or alternative splicing of downstream target genes remains unknown and warrants investigation.

Given the established role of PUM2 in fibrotic hearts of patients with dilated cardiomyopathy, whereby it acts as a translational hub for profibrotic genes, we hypothesized that it orchestrates MF through dual regulation of gene expression and alternative splicing in cardiomyocytes. In the present study, transcriptome data following knockdown of PUM2 in H9C2 rat cardiomyocytes were obtained via high-throughput sequencing. Potential transcriptional targets of PUM2 and alternative splicing in H9C2 cells were analyzed to investigate the molecular functions and mechanisms of PUM2 in the development of MF.

Materials and methods

Small interfering RNA (siRNA/si) information. For the present study, siRNA duplexes were sourced from Shanghai GenePharma Co., Ltd. A non-targeting control siRNA, labeled siNegative, was employed, with the following sequences: Sense, 5'-UUCUCCGAACGUGUCACGUTT-3' and antisense, 5'-ACGUGACACGUUCGGAGAATT-3'. Additionally, an siRNA designed specifically to target the PUM2 gene was employed, labeled siPUM2, with the following sequences: Sense, 5'-AGCAUUAGAAUCUAUUUCUUCUGAT-3' and antisense, 5-AUCAGAAGAAAUAGAUUCUAAUGCUUU-3.

Cell culture and transfection. H9C2 rat cardiomyocyte cells (cat. no. CL-0089; Procell Life Science & Technology Co., Ltd.) were cultured in a controlled environment at 37˚C with a humidified atmosphere containing 5% CO_2. The culture medium utilized was DMEM (cat. no. PM150210; Gibco; Thermo Fisher Scientific, Inc.), supplemented with 10% FBS (cat. no. 10091148; Gibco; Thermo Fisher Scientific, Inc.) and antibiotics including 100 μg/ml streptomycin and 100 U/ml penicillin (cat. no. SV30010; HyClone™; Cytiva). Cells in 12-well plates were transfected with 160 pmol siRNA using Lipofectamine™ RNAiMAX (cat. no. 13778150; Invitrogen; Thermo Fisher Scientific, Inc.) according to the manufacturer's protocol. Following a 48-h incubation at room temperature, the cells were harvested and analyzed by reverse transcription-quantitative PCR (RT-qPCR) and western blotting.

Assessment of gene expression. Total RNA was extracted from H9C2 cells by the TRIzol™ (Thermo Fisher Scientific, Inc.). The RNA was further purified with two phenol-chloroform treatments and then treated with RQ1 DNase (Promega Corporation) to remove DNA. The quality and quantity of the purified RNA were redetermined by measuring the absorbance at 260/280 nm (A260/A280) using NanoPhotometer N50 (Implen NanoPhotometers). The integrity of RNA was further verified by 1.0% agarose gel electrophoresis. cDNA was synthesized utilizing a reverse transcription kit (cat. no. R323-01; Vazyme Biotech Co., Ltd.). The procedure entailed an initial incubation at 42˚C for 5 min, followed by 15 min at 37˚C and a final step at 85˚C for 5 sec, all executed using the T100 thermocycler (Bio-Rad Laboratories, Inc.). Subsequent to cDNA synthesis, qPCR was conducted using the ABI QuantStudio™ 5 (conventional) system (Applied Biosystems; Thermo Fisher Scientific, Inc.). The amplification protocol included a denaturation step at 95˚C for 10 min, and 40 cycles comprising denaturation at 95˚C for 15 sec and a combined annealing and extension step at 60˚C for 1 min. Each sample was analyzed in triplicate to ensure data reliability. To quantify the expression levels of each transcript, normalization was performed using GAPDH, and the $2^{-\Delta\Delta Cq}$ method was used for data analysis (25). Detailed sequences of primers used for qPCR analysis are listed in Table SI.

Western blotting. H9C2 cells were lysed using ice-cold RIPA lysis buffer (cat. no. PR20001; Proteintech Group, Inc.) supplemented with protease inhibitors (cat. no. 4693116001; Sigma-Aldrich; Merck KGaA). The lysis process was carried

out on ice for 30 min to disrupt the cells while simultaneously inhibiting any protease activities that might lead to protein degradation. Following lysis, cell samples underwent a heating step, during which they were boiled for 10 min in conjunction with a protein loading buffer (cat. no. P1040; Beijing Solarbio Science & Technology Co., Ltd.). This heating step was key for denaturing the proteins, thereby facilitating their separation during subsequent analysis. Prepared samples (25 μg protein/lane) were then carefully loaded onto a 10% SDS-PAGE gel.Electrophoresis was carried out to separate the proteins based on their molecular weights, allowing for effective analysis of the protein profiles. Once electrophoresis was completed, the separated proteins were transferred onto 0.45-μm PVDF membranes (cat. no. ISEQ00010; MilliporeSigma) to enable further examination. Following successful protein transfer, the PVDF membrane was blocked with 5% skimmed milk to reduce non-specific binding. This involved incubating the membranes at room temperature for 1 h, which helped to minimize background noise during the detection phase. Subsequently, the membranes were incubated overnight at 4˚C with a specific primary GAPDH antibody (1:1,000; cat. no. A19056; ABclonal Biotech Co., Ltd.) that targeted PUM2 (1:1,000; cat. no. Ab92390; Abcam) and an actin antibody (1:1,000; cat. no. 20536-1-AP; Proteintech Group, Inc.). This overnight incubation allowed the primary antibodies time to bind to their respective protein targets. Following this incubation period, membranes were treated with an HRP-conjugated secondary antibody, either anti-rabbit (1:10,000; cat. no. SA00001-2; Proteintech Group, Inc.) or anti-mouse (1:10,000; cat. no. AS003; ABclonal Biotech Co., Ltd.), for 45 min at room temperature. This step was essential for enhancing the detection of the bound primary antibodies. Finally, visualization of the proteins on the membranes was achieved using an enhanced ECL reagent (BeyoECL Moon; cat. no. P0018FM; Beyotime Biotechnology), which permitted chemiluminescent detection of the proteins of interest.

Cell viability assay. In the present study, a cell viability assay was conducted utilizing a Cell Counting Kit-8 (CCK-8; Shanghai Yeasen Biotechnology Co., Ltd.). The procedure involved plating H9C2 cells at a density of 10,000 cells/well in 96-well culture plates in a controlled environment (37˚C and 5% CO_2) for cell viability. Cells were transfected with either a non-targeting control siRNA [negative control (NC) group] or dicer-substrate small interfering RNA (DSI; experimental group), while vials lacking cells served as blank controls to ensure measurement accuracy. Cells were incubated at 37˚C in a 5% CO_2 atmosphere for designated time periods: 48 and 72 h. Following incubation, 10 μl CCK-8 solution was added to each well for further incubation for 3 h at 37˚C. This step allowed for the assessment of cell viability. After incubation, the optical density (OD) was measured using the ELx800 microplate reader (BioTek; Agilent Technologies, Inc.) at a wavelength of 450 nm. To quantify the viability rate of the cells, the following formaul was applied: viability rate=(experimental OD value-blank OD value)/(control OD value-blank OD value) x100. This formula enabled a clear assessment of cell viability in response to varying treatments.

Flow cytometry analysis of apoptosis. For the assessment of apoptosis, an annexin V-allophycocyanin (APC)/7-aminoactinomycin D apoptosis detection kit (cat. no. 40304ES60; Shanghai Yeasen Biotechnology Co., Ltd.) was employed according to the manufacturer's instructions. H9C2 cells were cultivated in 6-well plates for 24 h at 37˚C and subsequently transfected with siRNAs for 48 h as aforementioned. The transfected and control siRNA cell populations were combined with 5 μl annexin V-APC and incubated in the dark at room temperature for 5 min, followed by the addition of 5 μl 7-amino-actinomycin for incubation for 5 min at room temperature. Samples were then analyzed using the BD FACSCanto™ Clinical Flow Cytometry system (BD Biosciences) to evaluate the levels of apoptosis, and the data were analyzed with FlowJo™ software (BD Biosciences).

RNA extraction and sequencing. Total RNA was isolated from H9C2 cells using TRIzol® reagent (cat. no. 15596026; Invitrogen; Thermo Fisher Scientific, Inc.), following the protocol established by Chomczynski and Sacchi (26). Following RNA extraction, DNA digestion (37˚C for 10 min) was carried out using RQ1 RNase-Free DNase (cat. no. M6101; Promega Corporation). RNA quality was assessed by measuring the A260/A280 ratio with a Nanodrop™ One^C spectrophotometer (Thermo Fisher Scientific, Inc.). Integrity was verified through 1.5% agarose gel electrophoresis. The concentration of selected RNA samples was subsequently quantified using the Qubit™ 3.0 fluorometer (Thermo Fisher Scientific, Inc.) in combination with the Qubit™ RNA broad range assay kit (cat. no. Q10210; Thermo Fisher Scientific, Inc.). A total of 2 μg RNA was then used for the preparation of stranded RNA-sequencing (RNA-seq) libraries, utilizing the KC™ Stranded mRNA Library Prep Kit for Illumina (cat. no. DR08402; Wuhan Kangce Technology) in accordance with the manufacturer's protocol. PCR products with lengths between 200 and 500 base pairs were enriched, quantified and ultimately sequenced by Novogene (Tianjin Sequencing Center and CAP Certified Clinical Lab, Tianjin, China) using the NovaSeq 6000 sequencer (Illumina, Inc.) and 150-bp paired-end sequencing was performed.

RNA-seq data and differentially expressed gene (DEG) analysis. Initially, raw sequencing reads that contained >2 ambiguous bases, denoted as 'N', were eliminated from the dataset to ensure data quality. Following this step, adaptors and low-quality base calls were systematically trimmed from the remaining raw sequencing reads. This processing was carried out using the FASTX-Toolkit (version 0.0.13; https://github.com/agordon/fastx_toolkit), which is specifically designed for efficient read preprocessing. Furthermore, any sequencing reads that were <16 nucleotides in length were discarded to maintain the integrity of the dataset. The clean reads that passed these quality control measures were then aligned to the mRatBN7.2 genome using the HISAT2 tool (v2.2.1; http://daehwankimlab.github.io/hisat2/), allowing for the accommodation of ≥4 mismatches during the alignment process. This alignment procedure ensured that the uniquely mapped reads could be accurately utilized for counting gene read numbers and for calculating the fragments per kilobase of transcript per million fragments mapped (FPKM). During analysis of gene

expression, the 'DESeq2' package (v 1.38.3; http://www.bioconductor.org/packages/release/bioc/html/DESeq2.html) from R Bioconductor (v 3.22; https://www.bioconductor.org/) was employed to identify DEGs using the thresholds P<0.01 and fold change >1.5 or <0.67. These parameters were essential for pinpointing variations in gene expression that could have biological relevance.

Alternative splicing analysis. For the analysis of alternative splicing events (ASEs) and specifically regulated ASEs (RASEs) among the samples, the ABLas pipeline (https://github.com/ablifedev/ablas) was employed. ABLas identifies 10 distinct forms of alternative splicing based on the analysis of splice junction reads. These forms include exon skipping (ES), intron retention (IntronR), alternative 5' splice sites (A5SS), alternative 3' splice sites (A3SS) and mutually exclusive exons (MXE), as well as variations in the 5' and 3' untranslated regions (UTRs), specifically mutually exclusive 5' UTRs and mutually exclusive 3' UTRs, in addition to cassette exons, and combinations of A3SS and ES, and A5SS and ES.

To evaluate the influence of PUM2 on the ASEs, statistical analysis was carried out using unpaired Student's t-test to determine the significance of changes in the ratio of ASEs across the samples. Events that demonstrated significant alterations, with a P-value corresponding to a threshold that aligned with a false discovery rate cut-off of 5%, were classified as PUM2-regulated ASEs. This approach ensured that only those events with statistical significance were recognized to be potentially influenced by PUM2.

RT-qPCR verification. For RT-qPCR verification with GAPDH as the control gene to measure relative target gene expression levels, total RNA was isolated from H9C2 cells using TRIzol reagent (cat. no. 15596026; Invitrogen; Thermo Fisher Scientific, Inc.). cDNA was synthesized with a reverse transcription kit (cat. no. R323-01; Vazyme Biotech Co., Ltd.) on a mycycler (cat. no. T100; Bio-Rad Laboratories, Inc.) at 42˚C for 5 min, 37˚C for 15 min and 85˚C for 5 sec. qPCR was performed on the ABI QuantStudio 5 with Hieff® qPCR SYBR Green Master Mix, starting with denaturing at 95˚C for 10 min, followed by 40 cycles of 95˚C for 15 sec and 60˚C for 1 min, with three technical replicates per sample. Transcript levels were normalized to GAPDH using the $2^{-\Delta\Delta Cq}$ method (25). The primers for pre-mRNA splicing detection, detailed in Table SI, were designed to target splice junctions between constitutive and alternative exons for precise isoform amplification.

Functional enrichment analysis. To organize the functional classifications of DEGs, the KOBAS 2.0 server (https://github.com/xmao/kobas) (19) was utilized to identify Gene Ontology (GO) terms as well as Kyoto Encyclopedia of Genes and Genomes (KEGG) pathways. The enrichment of each term was determined using the hyper-geometric test along with the Benjamini-Hochberg false discovery rate-controlling method.

Statistical analysis. All plots were conducted in R (version 4.2.3; https://cran.r-project.org/bin/windows/base/old/4.2.3/) as implemented in RStudio, in addition to pattern diagrams and stacked bar charts. Pattern diagrams and stacked bar charts were generated using GraphPad Prism (version 8.0; Dotmatics). Data are presented as the mean ± standard error of the mean (SEM), with three independent biological replicates. The statistical difference between two groups for the RT-qPCR, cell viability and apoptosis assays was calculated using an unpaired Student's t-test, where P<0.05 was considered to indicate a statistically significant difference. Other statistical methods used for the bioinformatics analyses have been described in the corresponding sections; for example, DEGs were calculated using DESeq2, and ASEs were analyzed using unpaired t-tests.

Results

Inhibition of viability in H9C2 cells by PUM2 knockdown. To explore the role of PUM2 in MF, H9C2 cell lines with PUM2 knockdown were constructed using siRNA transfection. Both RT-qPCR and western blotting confirmed successful knockdown of PUM2 in H9C2 cells (Fig. 1A and B). These efficiency validation experiments demonstrated that mRNA expression was significantly reduced (by ~50%) but not eliminated, whereas protein expression was knocked down; however, this was not statistically assessed. The rat PUM2 gene encodes five protein-coding transcripts, and the DSI sequence used may specifically target only a subset of these transcripts (27), while the RT-qPCR assay measured total PUM2 expression at the gene level. This selective targeting may explain why a larger reduction was observed at the protein level compared with the mRNA level. Consequently, expression from non-targeted transcripts masks the extent of knockdown in the PCR results, leading to the observed discrepancy between the RT-qPCR and western blot analyses. The effect of PUM2 knockdown on viability and apoptosis of H9C2 cells was detected using a CCK-8 assay and flow cytometry. The CCK-8 assay demonstrated that the viability of H9C2 cells was significantly inhibited at both 48 and 72 h after transfection following PUM2 knockdown (Fig. 1C). Flow cytometry revealed that PUM2 knockdown did not significantly affect apoptosis at 48 h post-transfection (Fig. S1). The results indicated that PUM2 is key for the regulation of viability in H9C2 cells.

PUM2 knockdown regulates gene expression in H9C2 cells. To explore the regulatory role of PUM2 in gene expression, RNA-seq was conducted to assess and compare the overall gene expression profiles between samples subjected to siPUM2 transfection and those in NC group. Utilizing the principal component method, the FPKM values of all DEGs were analyzed, with the first principal component (dimension 1) successfully distinguishing the DSI group from the control group (Fig. 2A). The volcano plot illustrates the DEGs identified between DSI and NC samples (Fig. 2B). A total of 147 DEGs influenced by PUM2 were identified, encompassing 95 upregulated and 52 downregulated genes. Additionally, analysis of the heat map depicting DEG expression patterns in the RNA-seq samples (Fig. 2C) revealed a high level of consistency among the three biological replicates regarding siPUM2-mediated transcription. Notably, the number of upregulated genes markedly exceeded that of downregulated genes, implying that PUM2 may exert a repressive effect on gene expression.

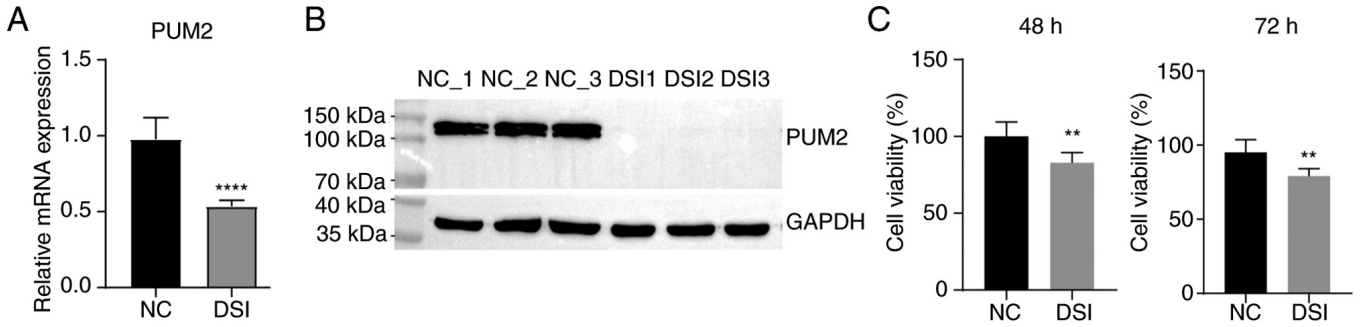

Figure 1. PUM2 knockdown inhibits viability in H9C2 cells. (A) Reverse transcription-quantitative PCR results after PUM2 knockdown. (B) Representative western blot bands after PUM2 knockdown. (C) PUM2 inhibited viability at 48 and 72 h after transfection. $^{**}P \leq 0.01$ and $^{****}P < 0.0001$. PUM2, pumilio RNA-binding family member 2; NC, negative control; DSI, dicer-substrate small interfering RNA.

To evaluate the possible biological functions of these DEGs, GO and KEGG enrichment analyses were conducted. GO enrichment analysis indicated that the genes exhibiting increased expression were predominantly associated with two pathways: 'Positive regulation of GTPase activity' and 'positive regulation of transcription from RNA polymerase II promoter' (Fig. S2). KEGG analysis provided comprehensive insights into the pathways associated with the upregulated genes, indicating their notable involvement in a multitude of key biological processes. The genes were heavily represented in pathways related to various forms of cardiomyopathy, such as 'hypertrophic cardiomyopathy', 'dilated cardiomyopathy' and 'arrhythmogenic right ventricular cardiomyopathy'. Additionally, analysis highlighted the inclusion of key signaling pathways, including the 'Rap1 signaling pathway' and the 'PI3K-Akt signaling pathway', both of which serve vital roles in cellular responses. Furthermore, the involvement of these genes in 'pathways in cancer', 'focal adhesion', the 'thyroid hormone signaling pathway', 'vascular smooth muscle contraction' and the 'Ras signaling pathway' underscores their relevance in the complex interplay of genetic and biochemical signals (Fig. 2D). Conversely, the examination of downregulated genes using GO enrichment analysis revealed a primary connection to 'positive regulation of cell proliferation' and 'positive regulation of transcription from RNA polymerase II promoter' (Fig. S2). KEGG analysis identified notable associations between the downregulated genes and a diverse array of biological pathways, including 'focal adhesion' and 'ECM-receptor interaction', both of which are key for cellular communication and structural integrity (28,29). Additionally, the 'PI3K-Akt signaling pathway' was revealed to serve a role in the regulation of these genes, along with pathways associated with 'arrhythmogenic right ventricular cardiomyopathy' and the 'regulation of the actin cytoskeleton'. Other notable associations included pathways involved in 'colorectal cancer', 'pantothenate and CoA biosynthesis', 'Parkinson disease' and 'human papillomavirus infection' (Fig. 2E). Specific pathways such as 'hypertrophic cardiomyopathy', 'dilated cardiomyopathy', 'arrhythmogenic right ventricular cardiomyopathy', 'vascular smooth muscle contraction', 'focal adhesion' (Fig. 2D), 'ECM-receptor interaction' and 'regulation of actin cytoskeleton' (Fig. 2E) are particularly noteworthy as they relate to molecular function. RNA-seq data for a representative set of five upregulated genes, including adrenomedullin (Adm), NDRG family member 4 (Ndrg4), phospholipid phosphatase 3 (Plpp3), integrin subunit α 8 (Itga8) and regulator of G protein signaling 2 (Rgs2), and three downregulated genes, including cadherin 11 (Cdh11), integrin subunit α 11 (Itga11) and transforming growth factor β-induced (Tgfbi), can be found in Fig. 2F.

Pathway analysis revealed that several significantly dysregulated genes are involved in key molecular functions. Notably, the elevated genes Itga8 and Adm, along with the downregulated gene Itga11 (identified in Tables I and II), were central components of the enriched pathways related to cell adhesion and cardiovascular regulation. To confirm the findings of RNA-seq, RT-qPCR was conducted to assess the relative expression patterns of the genes Adm, Itga8, Rgs2, Plpp3, Ndrg4, Itga11, Tgfbi and Cdh11 in both the control and experimental groups. Results from the RT-qPCR validation aligned with those obtained from the RNA-seq analysis, affirming the reliability of the sequencing data (Fig. 2F). RT-qPCR amplification and melting curves for all targets confirmed assay specificity and reproducibility, validating the RNA-seq findings (data not shown).

PUM2 regulates gene alternative splicing in H9C2 cells. To explore how PUM2 knockdown influences the regulation of alternative splicing, RNA-seq data were assessed to identify PUM2-regulated RASEs in the H9C2 cell line. The aforementioned ABLas pipeline was employed to characterize and quantify ASEs and RASEs across the different samples. The types and quantities of all notable RASEs between the NC and DSI samples are illustrated in Fig. 3A. The primary RASEs detected included IntronR (183 events), A3SS (129 events) and A5SS (100 events; Table SII). These findings indicate that PUM2 regulates ASEs globally in the H9C2 cell line. The heat map of splicing ratios for RASEs demonstrated high reproducibility across biological triplicates in siPUM2-treated cells (Fig. 3B). GO analysis of PUM2-regulated alternative splicing genes (PUM2-RAS) was carried out to explore the potential biological functions of PUM2-RAS. Analysis revealed that the enriched pathways included 'brain development', 'peptidyl-tyrosine dephosphorylation', 'axonogenesis', 'neural tube closure', 'mRNA processing', 'protein stabilization', 'positive regulation of GTPase activity', 'negative regulation of cell proliferation', 'protein phosphorylation' and 'cell proliferation' (Fig. 3C). Splicing ratios for several ASEs were significantly altered upon

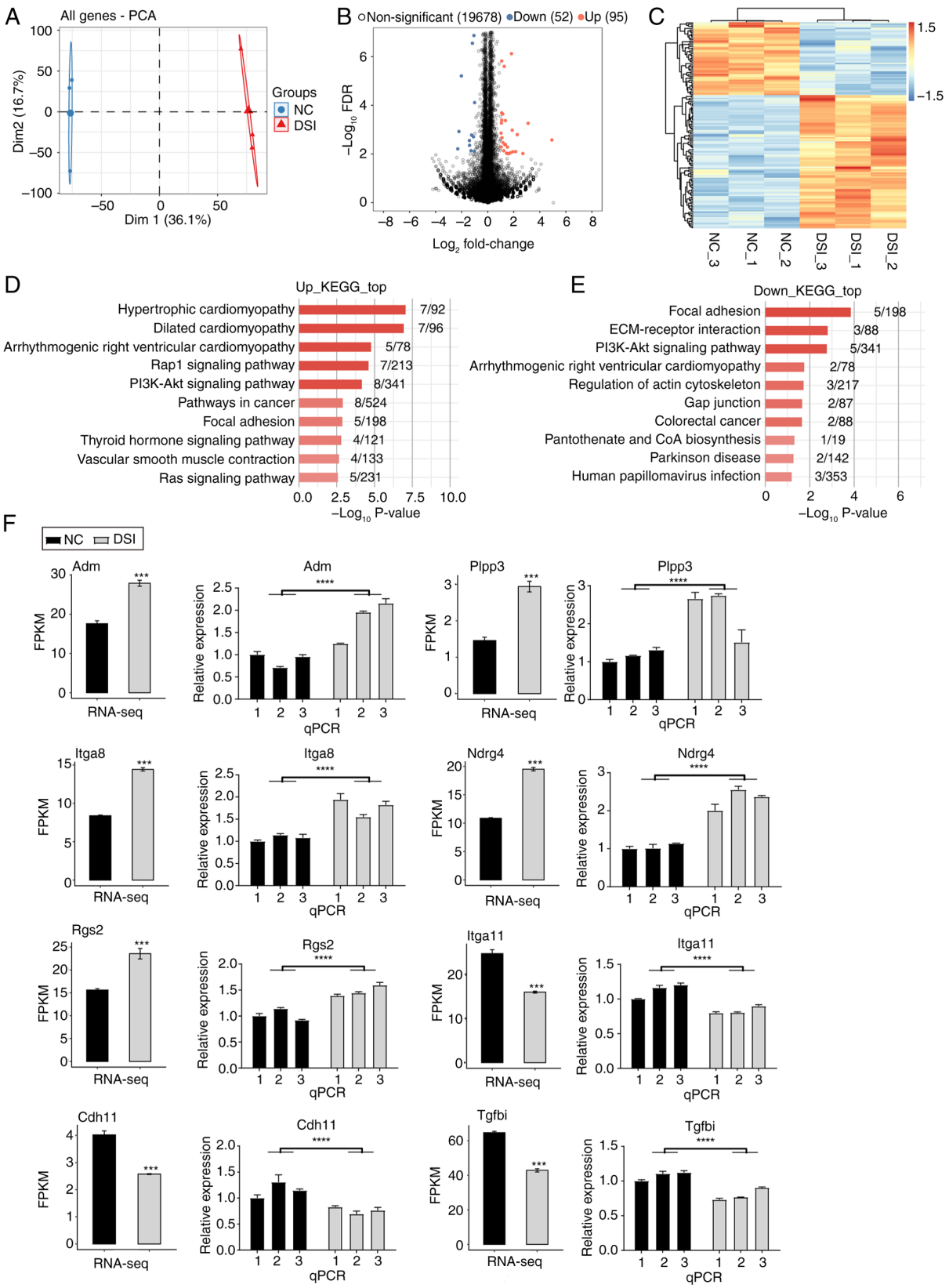

Figure 2. PUM2 knockdown regulates gene expression in H9C2 cells. (A) PCA based on the FPKM value of all genes. The ellipse for each group is the confidence ellipse. (B) Volcano plot showing all DEGs between DSI and NC samples. (C) Hierarchical clustering heat map showing expression levels of all DEGs. (D) Bar plot showing the enriched KEGG pathways of upregulated DEGs. (E) Bar plot showing the enriched KEGG pathways of downregulated DEGs. (F) Bar plots showing the expression pattern and statistical difference of DEGs with qPCR validation (numbers represent three biological replicate samples). Data are presented as the mean ± standard error of the mean. ***P<0.001 and ****P<0.0001. DSI, dicer-substrate small interfering RNA; PUM2, pumilio RNA-binding family member 2; PCA, principal component analysis; FPKM, fragments per kilobase of transcript per million fragments mapped; DEGs, differentially expressed genes; NC, negative control; KEGG, Kyoto Encyclopedia of Genes and Genomes; Adm, adrenomedullin; Itga8, integrin subunit α 8; RNA-seq, RNA-sequencing; Dim1, dimension 1; Dim2, dimension 2; FDR, false discovery rate; ECM, extracellular matrix; Rgs2, regulator of G protein signaling 2; Cdh11, cadherin 11; Plpp3, phospholipid phosphatase 3; Ndrg4, NDRG family member 4; Itga11, integrin subunit α 11; Tgfbi, transforming growth factor β-induced; qPCR, quantitative PCR.

Table I. Specific gene information for myocardial fibrosis-related pathways, as identified through Kyoto Encyclopedia of Genes and Genomes analysis of upregulated differentially expressed genes.

Term	Corrected P-value	Input
Hypertrophic cardiomyopathy	0.00000884	Itga8, Tnnt2, Atp2a1, Itga1, Sgcd, Prkaa2, Itga2b
Dilated cardiomyopathy	0.00000884	Itga8, Tnnt2, Atp2a1, Itga1, Sgcd, Itga2b, Pln
Arrhythmogenic right ventricular cardiomyopathy	0.00085372	Itga8, Itga1, Sgcd, Atp2a1, Itga2b
Vascular smooth muscle contraction	0.03787322	Myh1, Adm, Plcb4, Prkcg

Itga8, integrin subunit α 8; Tnnt2, troponin T2; Atp2a1, ATPase sarcoplasmic/endoplasmic reticulum Ca^{2+} transporting 1; Itga1, integrin subunit α 1; Sgcd, sarcoglycan δ; Prkaa2, protein kinase AMP-activated catalytic subunit α 2; Itga2b, integrin subunit α 2b; Pln, phospholamban; Myh11, myosin heavy chain 11; Adm, adrenomedullin; Plcb4, phospholipase C β-4; Prkcg, protein kinase C-γ.

Table II. Specific gene information linked to myocardial fibrosis-related pathways, as identified through Kyoto Encyclopedia of Genes and Genomes analysis of downregulated differentially expressed genes.

Term	Corrected P-value	Input
Focal adhesion	0.00968071	Col6a3, Pdgfb, Itga11, Mylpf, Tnc
ECM-receptor interaction	0.03893884	Col6a3, Itga11, Tnc
Arrhythmogenic right ventricular cardiomyopathy	0.21945932	Gja1, Itga11
Regulation of actin cytoskeleton	0.21945932	Pdgfb, Itga11, Mylpf

ECM, extracellular matrix; Col6a3, collagen type VI α 3 chain; Pdgfb, platelet derived growth factor subunit B; Itga11, integrin subunit α 11; Mylpf, myosin light chain 11; Tnc, tenascin C; Gja1, gap junction protein α 1.

PUM2 knockdown. Representative examples are presented in Figs. 3D and S3, including tropomyosin 1 (Tpm1; MXE), actinin a 1 (Actn1; ES) and PPFIA binding protein 1 (Ppfibp1; ES). The reads distribution diagram showed the distribution of splicing junctions for Tpm1 and Actn1, with significant changes in the splicing ratio (Fig. 3D). In addition, the distribution of Ppfibp1 is also represented as a reads distribution diagram, with the splicing ratio of Ppfibp1 presented as a bar plot (Fig. S3). RT-qPCR validation of ASEs in the Ppfibp1, Actn1 and Tpm1 genes aligned with the RNA-seq results (Figs. 3D and S3). RT-qPCR amplification and melting curves for all targets confirmed assay specificity and reproducibility, therefore validating the RNA-seq findings (data not shown).

Discussion

PUM2 is an abnormally expressed RBP in various diseases (30). However, its function and the corresponding mechanism of MF have not been fully explored. To the best of our knowledge, the present study was the first to investigate how PUM2 globally regulates the expression and alternative splicing of genes associated with MF in H9C2 cells. The present study examined the effects of PUM2 knockdown on gene expression levels and alternative splicing patterns in rat H9C2 cells using high-throughput transcriptome sequencing. Cytological experiment results indicated that PUM2 knockdown significantly inhibited the viability of H9C2 cells. RNA-seq results demonstrated that PUM2 knockdown led to 147 DEGs. Upregulation of the expression levels of Adm, Rgs2, Itga8, Plpp3 and Ndrg4 genes, as well as downregulation of the expression levels of Tgfbi, Itga11 and Cdh11 genes, was associated with the development of MF. Additionally, numerous ASEs were found in genes associated with fibrosis, such as Tpm1 (MXE) and Actn1 (ES). These results suggest that PUM2 can influence the development of MF by regulating the expression of associated genes and alternative splicing. PUM2 is a post-transcriptional regulator that controls numerous genes involved in key cellular pathways, including cell proliferation and differentiation (31). PUM2 has been shown to effectively inhibit translation and promote G_1 to S transition, resulting in a notable increase in cell proliferation (32). In addition, PUM2 has been identified as key in facilitating cardiomyocyte apoptosis induced by hypoxia or reoxygenation (33). By knocking down PUM2 in rat H9C2 cells and carrying out cytological analyses, the present study demonstrated that PUM2 is vital for the regulation of cell viability. Results indicated that silencing PUM2 markedly decreased cell viability without causing a notable change in apoptosis rates. These observations suggest that PUM2 is fundamental in modulating cell viability, primarily serving to enhance it, aligning with a previous study (32).

We hypothesized that PUM2 may contribute to the progression of MF by regulating the expression of MF-related genes. Therefore, the aim was to identify key genes involved in MF progression. RNA-seq analysis was conducted to identify DEGs between the DSI and control groups. The results demonstrated that PUM2 knockdown upregulated the expression levels of Adm, Itga8, Rgs2 and Plpp3 genes, which have been reported to be involved in the development of MF.

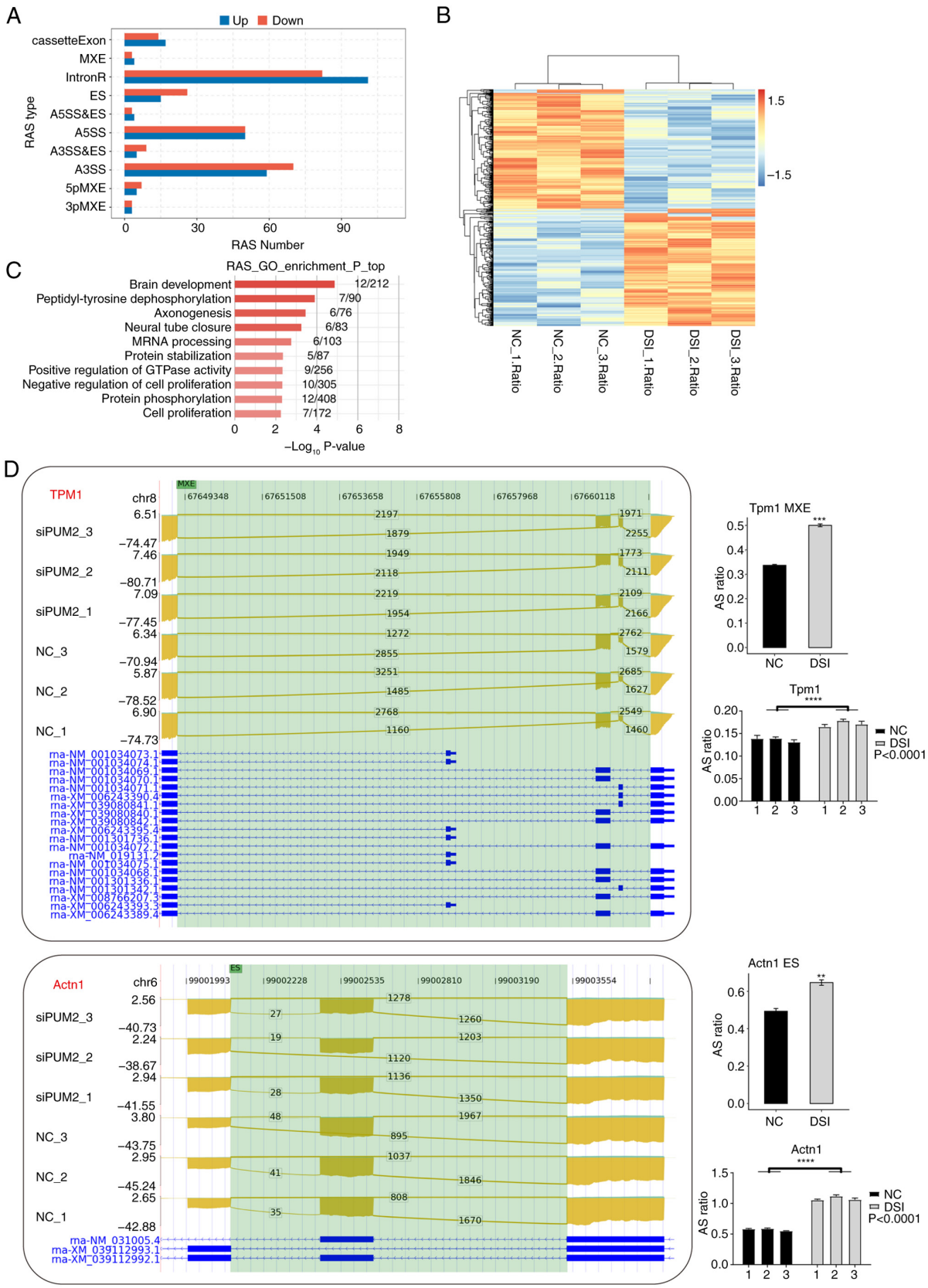

Figure 3. PUM2 regulates gene alternative splicing in H9C2 cells. (A) Bar plot showing the number of all notable regulated ASEs between DSI and NC samples. (B) Heat map of splicing ratios for ASEs with hierarchical clustering. (C) Bar plot showing the enriched GO biological process terms of RASG. (D) Reads distribution diagram showing Actn1 (ES) and Tpm1 (MXE). Green blocks indicate the positions where AS occurs (the connection lines above are junction reads and splicing sites). The top shows the absolute position of the chromosome base; the left side represents the samples, and the vertical coordinate is the normalized reads; the bottom provides transcript information. Bar plots showing splicing ratio of Actn1 (ES) and Tpm1 (MXE) and quantitative PCR validation. **P≤0.01, ***P≤0.001 and ****P<0.0001. DSI, dicer-substrate small interfering RNA; PUM2, pumilio RNA-binding family member 2; NC, negative control; ASE, alternative splicing event; GO, Gene Ontology, Actn1, actinin α1; ES, exon skipping; Tpm1, tropomyosin 1; MXE, mutually exclusive exon; intronR, intron retention; A5SS, alternative 5' splice sites; A3SS, alternative 3' splice sites; 3pMXE, mutually exclusive 3'UTRs; 5pMXE, mutually exclusive 5'UTRs; AS, alternative splicing; RASG, regulated alternative splicing gene.

The present study revealed notable upregulation of Adm in the 'vascular smooth muscle contraction pathway'. Adm, a multifunctional vasodilator peptide, reduces vascular tone and participates in hormone secretion and inflammatory responses (34). Adm may be a regulator of fibrosis development via multiple pathways (35-37). Furthermore, Adm expression has a protective effect against MF. Adm has been reported to inhibit fibroblast proliferation and ameliorate pressure overload-induced cardiac hypertrophy and MF (38). Igta8 is a cell surface protein belonging to the α-integrin family of transmembrane cell surface receptors (39). Igta8 was significantly enriched in the pathways of 'hypertrophic cardiomyopathy', 'dilated cardiomyopathy' and 'arrhythmogenic right ventricular cardiomyopathy'. Previous studies have found that aberrant Igta8 expression was associated with fibrosis (39,40).

In animals with angiotensin II (Ang II)-induced MF, the expression of integrin α8β1 has been shown to be increased in the left ventricle and arteries, suggesting that integrin α8β1 may contribute to the fibrotic process in the heart (41). In addition, Rgs2 is a multifunctional RGS protein involved in several G-protein signaling pathways (42). It regulates multiple cellular functions and behaviors in a range of cardiovascular cells (43). It has been shown that the expression of the Rgs2 gene is markedly associated with the pro-fibrotic effect induced by TGF-β1 in fibroblasts (44). In addition, Rgs2 serves a key role as a negative regulator of Ang II-induced cardiac fibroblast responses, thereby contributing to the development of Ang II-induced fibrosis (45). In addition, the Plpp3 gene is responsible for encoding lipid phosphate phosphatase 3 (LPP3), an enzyme that is integral to the membrane and functions to dephosphorylate glycerophospholipid and sphingolipid phosphate esters (46). LPP3 activity is key in vascular and cardiac development (47), and its expression regulates the differentiation state of vascular smooth muscle cells and influences fibroblast-like phenotypic transformation (48). Experimental evidence has demonstrated that, in a myeloid-specific Plpp3-deficient mouse model, the scar size and fibrosis area were markedly greater compared with those in controls 30 days after myocardial infarction (49). These findings indicate that PLPP3, responsible for encoding LPP3, may have a protective effect against MF.

PUM2 knockdown also upregulated the expression of the Ndrg4 gene. Ndrg4 is a member of the NDRG gene family, which is involved in cell proliferation, differentiation, development and the stress response (50). Research has revealed upregulation of Ndrg4 expression in liver fibrosis (51); however, there are limited studies on Ndrg4 in MF. DEGs that were downregulated, such as Itga11, Tgfbi and Cdh11, require further research regarding their involvement in the development of MF. The present study found that the downregulated gene Itga11 was a component of several fibrosis-related pathways identified by KEGG enrichment analysis, including 'focal adhesion', 'ECM-receptor interaction', 'arrhythmogenic right ventricular cardiomyopathy' and 'regulation of actin cytoskeleton. Additionally, research shows that Itgα11 is the primary collagen receptor on fibroblasts (52). Furthermore, the interaction between Itgα11 and TGF-β2 signaling has been found to promote myofibroblast differentiation in cardiac fibroblasts (53).

Tgfbi is an ECM protein that is upregulated by TGF-β1 (54) and is associated with the TGF-β1 pathway and cardiac fibrosis (55). In addition, Cdh11 is a type II cadherin that mediates calcium-dependent cell-cell adhesion (56). Cdh11 deficiency suppresses the activation and pro-fibrotic function of atrial fibroblasts, resulting in a reduction of atrial fibrosis (57). A previous study has demonstrated that cells expressing Cdh11 contribute to inflammation-driven fibrotic remodeling following myocardial infarction (58).

In the present study, after PUM2 knockdown, the expression levels of the Adm, Plpp3, Rgs2 and Itga8 genes were upregulated. The expression of Adm, Plpp3 and Rgs2 genes tends to be protective against MF, whereas Igta8 may exacerbate MF. Based on the findings of the present study, it is proposed that the effects of PUM2 on MF are the result of a combination of global gene regulatory networks of PUM2. Future research endeavors should focus on a comprehensive analysis of the molecular functions associated with each specific target gene. Additionally, it is essential to examine the context-dependent interactions that arise from PUM2-mediated global modifications within a signaling pathway. Such an approach will contribute to a deeper understanding of the mechanisms through which PUM2 influences the development of MF. By integrating these two perspectives, the intricate relationships and dynamics at play can be explored, ultimately leading to a more complete evaluation of the role of PUM2 in MF progression.

In the regulation of RBPs at the post-transcriptional level, alternative splicing is essential. This entails rearranging the exons of pre-mRNA in various configurations to generate mRNA and protein variants that differ structurally and functionally (59). This mechanism is closely monitored, as non-coding regions of pre-mRNA are eliminated while protein-coding parts are combined (60). Consequently, this approach leads to the formation of proteins that exhibit distinct or even opposing functionalities. The present study proposes that PUM2 could have a notable influence on post-transcriptional regulation, with a specific focus on alternative splicing. Analysis revealed that PUM2 affected a large number of ASEs in the H9C2 cell line. Specifically, ≥530 transcripts were found to be regulated by PUM2. The majority of the RASEs identified in the present study were classified as IntronR (183 events), A3SS (129 events) and A5SS (100 events). Importantly, a number of ASEs were found in genes associated with fibrosis, including Tpm1 and Actn1. Tpm1 is involved in the development of various cardiac diseases, such as hypertrophic and dilated cardiomyopathies (61,62), and it has been suggested that cardiac fibrosis is notably reduced after specific mutations in the lysine crotonylation locus of Tpm1 (63). In addition, Actn1 is a cytoskeletal protein that serves an important role in mediating sarcomere function (64). Actn1 could be an additional potential marker for myofibroblasts (65); however, its role in MF remains to be investigated. Ppfibp11, also known as liprin-β1, is a ubiquitously expressed liprin (66) that may be associated with an inflammatory myofibroblastic tumor (67). To the best of our knowledge, limited reports exist regarding the involvement of Ppfibp1 in fibrosis.

The present study, based on the alternative splicing data, suggested that PUM2 may affect the progression of MF by regulating the alternative splicing of genes such as Tpm1

and Actn1. The aim of the present study was to investigate PUM2-mediated ASEs, which are important post-transcriptional regulatory mechanisms involved in the development of MF. These ASEs may serve as important biomarkers and potential therapeutic targets for MF. Although the global catalog of PUM2-RASEs was identified, further studies are necessary to investigate the molecular consequences of the affected transcripts. This will aid in understanding the molecular functions of the affected genes and the PUM2-mediated context-dependent regulatory network of ASEs.

PUM2 knockdown orchestrates multi-pathway anti-fibrotic effects through coordinated transcriptional and post-transcriptional regulation. Specifically, suppression of the TGF-β pathway occurs through regulator of G-protein signaling 2 upregulation, which inhibits G q protein α subunit-mediated TGF-β receptor signaling (45), combined with Tgfbi downregulation that reduces ECM-bound TGF-β1 bioavailability (55), collectively attenuating SMAD2/3 phosphorylation and fibroblast-to-myofibroblast transition. Concurrently, integrin-cytoskeleton integrity is compromised through Itga11 downregulation, impairing αvβ6 integrin-dependent latent TGF-β activation, collagen I binding (68) and aberrant Actn1 splicing that generates isoforms deficient in Z-disc binding domains, ultimately disrupting mechanical force transmission and focal adhesion complex assembly (64). Furthermore, coordinated reduction of Cdh11 (diminishing cadherin-mediated fibroblast aggregation) and Tgfbi (suppressing matricellular signaling) synergistically limits fibrotic niche formation, indicating the regulation of ECM remodeling by PUM2 (56).

A key limitation of the present study is that while H9C2 cells provide a tractable model for initial mechanistic insights, they lack the multicellular interactions (such as cardiomyocyte-fibroblast crosstalk) and hemodynamic stressors present *in vivo*. Future studies should aim to validate the role of PUM2 in pressure-overload murine models (such as transverse aortic constriction) and human cardiac fibroblasts. Additionally, the functional impact of PUM2-regulated splicing events (such as Tpm1 MXE) on protein isoform activity warrants investigation through isoform-specific knockdown. Despite these limitations, the identification of PUM2 as a global regulator of MF-associated transcripts and splicing events nominates it as a potential therapeutic node. Pharmacological inhibition of PUM2 (for example, using antisense oligonucleotides) could simultaneously target multiple fibrotic pathways, overcoming the redundancy that limits single-target approaches.

In conclusion, the properties of PUM2 as an RBP suggest that it may have a multifunctional role in post-transcriptional RNA regulation. In the present study, RNA-seq was used to investigate the role of PUM2 in the H9C2 cell line and it was concluded that it may contribute to the development of MF by regulating the expression and alternative splicing of related genes. The present study indicated that PUM2 was associated with the development of MF and partially explained its molecular mechanisms. Further molecular investigations of the target genes of PUM2, as identified by the present RNA-seq experiment, could aid in the development of PUM2 as a therapeutic target for MF.

Acknowledgements

Not applicable.

Funding

The People's Hospital of Xinjiang Uygur Autonomous Region (grant no. 20210208) funded the present study.

Availability of data and materials

The data generated in the present study may be found in the (Gene Expression Omnibus database) under accession number (GSE302720) or at the following URL: https://www.ncbi.nlm.nih.gov/geo/query/acc.cgi?acc=GSE302720. The remaining data generated in the present study may be requested from the corresponding author.

Authors' contributions

The present study was conceived and designed by both JL and ZW. JL and ZW confirm the authenticity of all the raw data. The majority of the experiments and data analysis were carried out by ZZ and HZ, who also drafted the initial manuscript. Data collection was carried out by WZhu, DA, YL and WZho, who also contributed to the drafting of the manuscript. All authors read and approved the final version of the manuscript.

Ethics approval and consent to participate

Not applicable.

Patient consent for publication

Not applicable.

Competing interests

The authors declare that they have no competing interests.

References

1. Tian G and Ren T: Mechanical stress regulates the mechano-transduction and metabolism of cardiac fibroblasts in fibrotic cardiac diseases. Eur J Cell Biol 102: 151288, 2023.
2. Frangogiannis NG: Cardiac fibrosis. Cardiovasc Res 117: 1450-1488, 2021.
3. Zou Y, Shi H, Li Y, Li T, Liu N and Liu B: Heat shock protein 27 downregulation attenuates isoprenaline-induced myocardial fibrosis and diastolic dysfunction by modulating the endothelial-mesenchymal transition. Biochem Pharmacol 230: 116612, 2024.
4. Li C, Wang N, Rao P, Wang L, Lu D and Sun L: Role of the microRNA-29 family in myocardial fibrosis. J Physiol Biochem 77: 365-376, 2021.
5. Disertori M, Masè M and Ravelli F: Myocardial fibrosis predicts ventricular tachyarrhythmias. Trends Cardiovas Med 27: 363-372, 2017.
6. Zhao X, Kwan JYY, Yip K, Liu PP and Liu FF: Targeting metabolic dysregulation for fibrosis therapy. Nat Rev Drug Discov 19: 57-75, 2020.
7. Fang Z, Raza U, Song J, Lu J, Yao S, Liu X, Zhang W and Li S: Systemic aging fuels heart failure: Molecular mechanisms and therapeutic avenues. ESC Heart Fail 12: 1059-1080, 2025.
8. Liu M, López de Juan Abad B and Cheng K: Cardiac fibrosis: Myofibroblast-mediated pathological regulation and drug delivery strategies. Adv Drug Deliver Rev 173: 504-519, 2021.

9. Galeș LN, Păun MA, Butnariu I, Simion L, Manolescu LSC, Trifănescu OG and Anghel RM: Next-Generation sequencing in oncology-a guiding compass for targeted therapy and emerging applications. Int J Mol Sci 26: 3123, 2025.
10. Waarts MR, Stonestrom AJ, Park YC and Levine RL: Targeting mutations in cancer. J Clin Invest 132: e154943, 2022.
11. Wang S, Sun Z, Lei Z and Zhang HT: RNA-binding proteins and cancer metastasis. Semin Cancer Biol 86: 748-768, 2022.
12. Gebauer F, Schwarzl T, Valcárcel J and Hentze MW: RNA-binding proteins in human genetic disease. Nat Rev Genet 22: 185-198, 2021.
13. Chen X, Wu J, Li Z, Han J, Xia P, Shen Y, Ma J, Liu X, Zhang J and Yu P: Advances in the study of RNA-binding proteins in diabetic complications. Mol Metab 62: 101515, 2022.
14. Smith JM, Sandow JJ and Webb AI: The search for RNA-binding proteins: A technical and interdisciplinary challenge. Biochem Soc Trans 49: 393-403, 2021.
15. Hu X, Wu P, Liu B, Lang Y and Li T: RNA-binding protein CELF1 promotes cardiac hypertrophy via interaction with PEBP1 in cardiomyocytes. Cell Tissue Res 387: 111-121, 2022.
16. Zhu H, Zhang Y, Zhang C and Xie Z: RNA-binding profiles of CKAP4 as an RNA-binding protein in myocardial tissues. Front Cardiovasc Med 8: 773573, 2021.
17. Chen Z, He C, Gao Z, Li Y, He Q, Wang Y and Cai C: Polypyrimidine tract binding protein 1 exacerbates cardiac fibrosis by regulating fatty acid-binding protein 5. ESC Heart Fail 10: 1677-1688, 2023.
18. Wang D, Ruan X, Liu X, Xue Y, Shao L, Yang C, Zhu L, Yang Y, Li Z, Yu B, *et al*: SUMOylation of PUM2 promotes the vasculogenic mimicry of glioma cells via regulating CEBPD. Clin Transl Med 10: e168, 2020.
19. D'Amico D, Mottis A, Potenza F, Sorrentino V, Li H, Romani M, Lemos V, Schoonjans K, Zamboni N, Knott G, *et al*: The RNA-binding protein PUM2 impairs mitochondrial dynamics and mitophagy during aging. Mol Cell 73: 775-787.e10, 2019.
20. Ding Y, Yuan X and Gu W: Circular RNA RBM33 contributes to cervical cancer progression via modulation of the miR-758-3p/PUM2 axis. J Mol Histol 52: 173-185, 2021.
21. Liu Q, Liu Y, Li Y, Hong Z, Li S and Liu C: PUM2 aggravates the neuroinflammation and brain damage induced by ischemia-reperfusion through the SLC7A11-dependent inhibition of ferroptosis via suppressing the SIRT1. Mol Cell Biochem 478: 609-620, 2023.
22. Gibb AA, Lazaropoulos MP and Elrod JW: Myofibroblasts and fibrosis: Mitochondrial and metabolic control of cellular differentiation. Circ Res 127: 427-447, 2020.
23. Tsoy S and Liu J: Regulation of protein synthesis at the translational level: Novel findings in cardiovascular biology. Biomolecules 15: 692, 2025.
24. Chothani S, Schäfer S, Adami E, Viswanathan S, Widjaja AA, Langley SR, Tan J, Wang M, Quaife NM, Jian Pua C, *et al*: Widespread translational control of fibrosis in the human heart by RNA-binding proteins. Circulation 140: 937-951, 2019.
25. Livak KJ and Schmittgen TD: Analysis of relative gene expression data using real-time quantitative PCR and the 2(-Delta Delta C(T)) method. Methods 25: 402-408, 2001.
26. Chomczynski P and Sacchi N: Single-step method of RNA isolation by acid guanidinium thiocyanate-phenol-chloroform extraction. Anal Biochem 162: 156-159, 1987.
27. Zhou Y, Ng DY, Richards AM and Wang P: Loss of full-length pumilio 1 abrogates miRNA-221-induced gene p27 silencing-mediated cell proliferation in the heart. Mol Ther Nucleic Acids 27: 456-470, 2021.
28. Tapial Martinez P, López Navajas P and Lietha D: FAK structure and regulation by membrane interactions and force in focal adhesions. Biomolecules 10: 179, 2020.
29. Martisova A, Sommerova L, Krejci A, Selingerova I, Kolarova T, Zavadil Kokas F, Holanek M, Podhorec J, Kazda T and Hrstka R: Identification of AGR2 gene-specific expression patterns associated with epithelial-mesenchymal transition. Int J Mol Sci 23: 10845, 2022.
30. Smialek MJ, Ilaslan E, Sajek MP and Jaruzelska J: Role of PUM RNA-binding proteins in cancer. Cancers (Basel) 13: 129, 2021.
31. Galgano A, Forrer M, Jaskiewicz L, Kanitz A, Zavolan M and Gerber AP: Comparative analysis of mRNA targets for human PUF-family proteins suggests extensive interaction with the miRNA regulatory system. PLoS One 3: e3164, 2008.
32. Lin K, Qiang W, Zhu M, Ding Y, Shi Q, Chen X, Zsiros E, Wang K, Yang X, Kurita T and Xu EY: Mammalian Pum1 and Pum2 control body size via translational regulation of the cell cycle inhibitor Cdkn1b. Cell Rep 26: 2434-2450.e6, 2019.
33. Cao Y, Liu C, Wang Q, Wang W, Tao E and Wan L: Pum2 mediates Sirt1 mRNA decay and exacerbates hypoxia/reoxygenation-induced cardiomyocyte apoptosis. Exp Cell Res 393: 112058, 2020.
34. Wong HK, Tang F, Cheung TT and Cheung BM: Adrenomedullin and diabetes. World J Diabetes 5: 364-371, 2014.
35. Wei Y, Tanaka M, Sakurai T, Kamiyoshi A, Ichikawa-Shindo Y, Kawate H, Cui N, Kakihara S, Zhao Y, Aruga K, *et al*: Adrenomedullin ameliorates pulmonary fibrosis by regulating TGF-ß-smads signaling and myofibroblast differentiation. Endocrinology 162: bqab090, 2021.
36. Kach J, Sandbo N, Sethakorn N, Williams J, Reed EB, La J, Tian X, Brain SD, Rajendran K, Krishnan R, *et al*: Regulation of myofibroblast differentiation and bleomycin-induced pulmonary fibrosis by adrenomedullin. Am J Physiol Lung Cell Mol Physiol 304: L757-L764, 2013.
37. Nagae T, Mori K, Mukoyama M, Kasahara M, Yokoi H, Suganami T, Sawai K, Yoshioka T, Koshikawa M, Saito Y, *et al*: Adrenomedullin inhibits connective tissue growth factor expression, extracellular signal-regulated kinase activation and renal fibrosis. Kidney Int 74: 70-80, 2008.
38. Niu P, Shindo T, Iwata H, Iimuro S, Takeda N, Zhang Y, Ebihara A, Suematsu Y, Kangawa K, Hirata Y and Nagai R: Protective effects of endogenous adrenomedullin on cardiac hypertrophy, fibrosis, and renal damage. Circulation 109: 1789-1794, 2004.
39. Hung CF, Wilson CL, Chow YH and Schnapp LM: Role of integrin alpha8 in murine model of lung fibrosis. PLoS One 13: e0197937, 2018.
40. Levine D, Rockey DC, Milner TA, Breuss JM, Fallon JT and Schnapp LM: Expression of the integrin alpha8beta1 during pulmonary and hepatic fibrosis. Am J Pathol 156: 1927-1935, 2000.
41. Bouzeghrane F, Mercure C, Reudelhuber TL and Thibault G: Alpha8beta1 integrin is upregulated in myofibroblasts of fibrotic and scarring myocardium. J Mol Cell Cardiol 36: 343-353, 2004.
42. Kehrl JH and Sinnarajah S: RGS2: A multifunctional regulator of G-protein signaling. Int J Biochem Cell Biol 34: 432-438, 2002.
43. Zhang P and Mende U: Functional role, mechanisms of regulation, and therapeutic potential of regulator of G protein signaling 2 in the heart. Trends Cardiovasc Med 24: 85-93, 2014.
44. Wu X, Gou H, Zhou O, Qiu H, Liu H, Fu Z and Chen L: Human umbilical cord mesenchymal stem cells combined with pirfenidone upregulates the expression of RGS2 in the pulmonary fibrosis in mice. Respir Res 23: 270, 2022.
45. Zhang P, Su J, King ME, Maldonado AE, Park C and Mende U: Regulator of G protein signaling 2 is a functionally important negative regulator of angiotensin II-induced cardiac fibroblast responses. Am J Physiol Heart Circ Physiol 301: H147-H156, 2011.
46. Mao G, Smyth SS and Morris AJ: Regulation of PLPP3 gene expression by NF-κB family transcription factors. J Biol Chem 294: 14009-14019, 2019.
47. Busnelli M, Manzini S, Parolini C, Escalante-Alcalde D and Chiesa G: Lipid phosphate phosphatase 3 in vascular pathophysiology. Atherosclerosis 271: 156-165, 2018.
48. Van Hoose PM, Yang L, Kraemer M, Ubele M, Morris AJ and Smyth SS: Lipid phosphate phosphatase 3 in smooth muscle cells regulates angiotensin II-induced abdominal aortic aneurysm formation. Sci Rep 12: 5664, 2022.
49. Tripathi H, Shindo K, Donahue RR, Gao E, Kuppa A, ElKammar M, Morris AJ, Smyth SS and Abdel-Latif A: Myeloid-specific deletion of lipid Plpp3 (phosphate phosphatase 3) increases cardiac inflammation after myocardial infarction. Arterioscler Thromb Vasc Biol 43: 379-381, 2023.
50. Melotte V, Qu X, Ongenaert M, van Criekinge W, de Bruïne AP, Baldwin HS and van Engeland M: The N-myc downstream regulated gene (NDRG) family: Diverse functions, multiple applications. FASEB J 24: 4153-4166, 2010.
51. Gibriel AA, Ismail MF, Sleem H, Zayed N, Yosry A, El-Nahaas SM and Shehata NI: Diagnosis and staging of HCV associated fibrosis, cirrhosis and hepatocellular carcinoma with target identification for miR-650, 552-3p, 676-3p, 512-5p and 147b. Cancer Biomark 34: 413-430, 2022.
52. Popova SN, Barczyk M, Tiger CF, Beertsen W, Zigrino P, Aszodi A, Miosge N, Forsberg E and Gullberg D: Alpha11 beta1 integrin-dependent regulation of periodontal ligament function in the erupting mouse incisor. Mol Cell Biol 27: 4306-4316, 2007.
53. Talior-Volodarsky I, Connelly KA, Arora PD, Gullberg D and McCulloch CA: α11 integrin stimulates myofibroblast differentiation in diabetic cardiomyopathy. Cardiovasc Res 96: 265-275, 2012.

54. Lee SG, Chae J, Woo SM, Seo SU, Kim HJ, Kim SY, Schlaepfer DD, Kim IS, Park HS, Kwon TK and Nam JO: TGFBI remodels adipose metabolism by regulating the Notch-1 signaling pathway. Exp Mol Med 55: 520-531, 2023.
55. Gao QY, Zhang HF, Chen ZT, Li YW, Wang SH, Wen ZZ, Xie Y, Mai JT, Wang JF and Chen YX: Construction and analysis of a ceRNA network in cardiac fibroblast during fibrosis based on in vivo and in vitro data. Front Genet 11: 503256, 2021.
56. Ruan W, Pan R, Shen X, Nie Y and Wu Y: CDH11 promotes liver fibrosis via activation of hepatic stellate cells. Biochem Biophys Res Commun 508: 543-549, 2019.
57. Cao W, Song S, Fang G, Li Y, Wang Y and Wang QS: Cadherin-11 deficiency attenuates Ang-II-induced atrial fibrosis and susceptibility to atrial fibrillation. J Inflamm Res 14: 2897-2911, 2021.
58. Schroer AK, Bersi MR, Clark CR, Zhang Q, Sanders LH, Hatzopoulos AK, Force TL, Majka SM, Lal H and Merryman WD: Cadherin-11 blockade reduces inflammation-driven fibrotic remodeling and improves outcomes after myocardial infarction. JCI Insight 4: e131545, 2019.
59. Fu XD and Ares M Jr: Context-dependent control of alternative splicing by RNA-binding proteins. Nat Rev Genet 15: 689-701, 2014.
60. Li WJ, Huang Y, Lin YA, Zhang BD, Li MY, Zou YQ, Hu GS, He YH, Yang JJ, Xie BL, *et al*: Targeting PRMT1-mediated SRSF1 methylation to suppress oncogenic exon inclusion events and breast tumorigenesis. Cell Rep 42: 113385, 2023.
61. Lorenzini M, Norrish G, Field E, Ochoa JP, Cicerchia M, Akhtar MM, Syrris P, Lopes LR, Kaski JP and Elliott PM: Penetrance of hypertrophic cardiomyopathy in sarcomere protein mutation carriers. J Am Coll Cardiol 76: 550-559, 2020.
62. Rajan S, Jagatheesan G, Petrashevskaya N, Biesiadecki BJ, Warren CM, Riddle T, Liggett S, Wolska BM, Solaro RJ and Wieczorek DF: Tropomyosin pseudo-phosphorylation results in dilated cardiomyopathy. J Biol Chem 294: 2913-2923, 2019.
63. Cai W, Xu D, Zeng C, Liao F, Li R, Lin Y, Zhao Y, Dong W, Wang Q, Yang H, *et al*: Modulating lysine crotonylation in cardiomyocytes improves myocardial outcomes. Circ Res 131: 456-472, 2022.
64. Xie GF, Zhao LD, Chen Q, Tang DX, Chen QY, Lu HF, Cai JR and Chen Z: High ACTN1 is associated with poor prognosis, and ACTN1 silencing suppresses cell proliferation and metastasis in oral squamous cell carcinoma. Drug Des Devel Ther 14: 1717-1727, 2020.
65. Wettlaufer SH, Scott JP, McEachin RC, Peters-Golden M and Huang SK: Reversal of the transcriptome by prostaglandin E2 during myofibroblast dedifferentiation. Am J Respir Cell Mol Biol 54: 114-127, 2016.
66. Dong C, Li X, Yang J, Yuan D, Zhou Y, Zhang Y, Shi G, Zhang R, Liu J, Fu P and Sun M: PPFIBP1 induces glioma cell migration and invasion through FAK/Src/JNK signaling pathway. Cell Death Dis 12: 827, 2021.
67. Yoshida A, Shibata T, Tsuta K, Watanabe SI and Tsuda H: Inflammatory myofibroblastic tumour of the lung with a novel PPFIBP1-ALK fusion variant. Histopathology 63: 881-883, 2013.
68. Diehl P, Fricke A, Sander L, Stamm J, Bassler N, Htun N, Ziemann M, Helbing T, El-Osta A, Jowett JB and Peter K: Microparticles: Major transport vehicles for distinct microRNAs in circulation. Cardiovasc Res 93: 633-644, 2012.